Supporting Information

for

Concentration Gradient Induced Delithiation Failure of MoO_3 for Li-ion Batteries

Jihyun Jang[1], Hyun-seung Kim[2], San Moon[3], Oh B. Chae[1], Sung-Jin Ahn[4], Heechul Jung[5], Junghyun Choi[6], Seung M. Oh[1], Ji Heon Ryu[7], and Taeho Yoon[8]**

[1]Department of Chemical and Biological Engineering, Seoul National University, Seoul, 08826, Republic of Korea

[2]Advanced Batteries Research Center, Korea Electronic Technology Institute, Seongnam, 13509, Republic of Korea

[3]Energy Material Research Center, Korea Research Institute of Chemical Technology, Daejeon, 34114, Republic of Korea

[4]Samsung Advanced Institute of Technology, Suwon, 16678, Republic of Korea

[5]Energy and Mineral Resources Engineering, Dong-A University, Busan, 49315, Republic of Korea

[6]Energy Storage Materials Center, Energy & Environmental Division, Korea Institute of Ceramic Engineering & Technology, Jinju, 52852, Republic of Korea

[7]Graduate School of Knowledge-based Technology and Energy, Korea Polytechnic University, Siheung, 15073, Republic of Korea

[8]School of Chemical Engineering, Yeungnam University, Gyeongsan, 38541, Republic of Korea

Corresponding Author: J. H. Ryu: ryujh@kpu.ac.kr, T. Yoon: tyoon@yu.ac.kr

Experimental Section

Material preparation: Highly crystalline microscale MoO_3 powder was prepared by a solid-state synthesis reaction. Ammonium heptamolybdate tetrahydrate ($(NH_4)_6Mo_7O_{24}•4H_2O$; 81–83 %, Alfa, USA) was heated at 600 °C for 10 h in air to produce MoO_3. The obtained MoO_3 was ball-milled, using a planetary ball mill (Planetary Micro Mill PULVERISETTE 7 premium line, FRITSCH, Germany), at a low speed (300 rpm) to minimize the changes in the Mo oxidation state in MoO_3. Ball milling was performed for 0 min (pristine), 5 min, 30 min, 2 h, and 4 h. Next, the pristine and 30 min ball-milled MoO_3 electrodes were examined by electrochemical and spectroscopic methods. In addition, nanoscale MoO_3 particles with diameters of hundreds of nanometers were synthesized through a solid-state reaction at 500 °C, with the same heating time and environment as the sample prepared at 600 °C.

Electrode fabrication: The composite electrodes were fabricated by mixing the active material, Super P (carbon black) and carboxymethyl cellulose (CMC, binder) at a weight ratio of 80:10:5. The active material and Super P were mixed with a CMC solution (1.2 *wt.*% in distilled water) to obtain a slurry. Then, 5 wt.% of styrene butadiene resin was added to the slurry to enhance the binding ability. Finally, the slurry was coated on a copper foil and the electrode was vacuum dried at 120 °C for 12 h.

Electrochemical characterization: The electrochemical performance was evaluated using a two-electrode 2032-type coin cell. The electrolyte was 1.0 M $LiPF_6$, dissolved in a mixture of ethylene carbonate and diethyl carbonate (1:1, volume ratio). A porous polypropylene (PP) – polyethylene – PP multilayer film was used as the separator. Galvanostatic charge/discharge experiments were conducted at a current density of 100 mA g^{-1}, over a voltage range of 0–3 V (*vs.* Li/Li^+), in a temperature-controlled oven (25 °C). For complete charging (lithiation), a constant voltage step at 0 V (*vs.* Li/Li^+) was added until the current density decayed to 10 mA g^{-1}. Cycle performances were evaluated at a current density of 500 mA g^{-1}. The GITT experiments were conducted during 10 min charge/discharge and 50 min rest with the same voltage and current conditions in the galvanostatic cycling.

Physical analysis: The particle size, morphology, and surface area of the ball-milled MoO_3 powders were examined by FE-SEM (JEOL JSM-6700F, Japan), TEM (JEOL JEM-3010, Japan), and BET method (Micromeritics analyzer, ASAP 2000, USA). The XRD patterns were obtained using Cu K_α radiation (1.54056 Å) with a D8-Bruker diffractometer (Bruker, Germany), operated at 40 kV and 40 mA with continuous scanning at a rate of 5° min^{-1}. To estimate the change in the oxidation state of MoO_3 after long-term ball milling, TGA (TA Instrument Q600 analyzer, USA) was performed in air or under N_2 environments, with a heating rate of 10 °C min^{-1}. The change in the Mo valency during the charging/discharging was examined via the Mo K-edge XANES spectra, obtained at the 7D XAFS beamline at the Pohang Light Source, with a ring current of 120–170 mA at 2.5 GeV. The energy of the Mo absorption edge was calibrated using the spectrum of a thin film of Mo metal as the reference. XPS (Sigma probe, USA) was conducted via Al-K_α (1486.6 eV) X-ray radiation produced at a constant power of 100 W (15 kV and 6.67 mA) with a spot radius of 200 μm and the pass energy for the detector of 30 eV.

Computational simulation: The governing equation, initial and boundary conditions, and parameters are presented in Table S1. The differential equation was solved using a numerical solver embedded in the software, MATLAB R2020b.

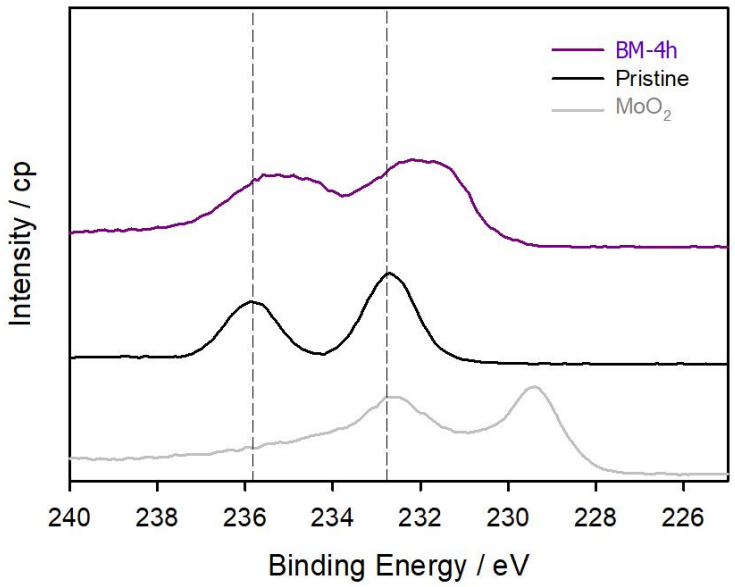

Figure S1. Mo 3d XPS spectra of MoO_2, pristine (MoO_3), and BM-4h samples.

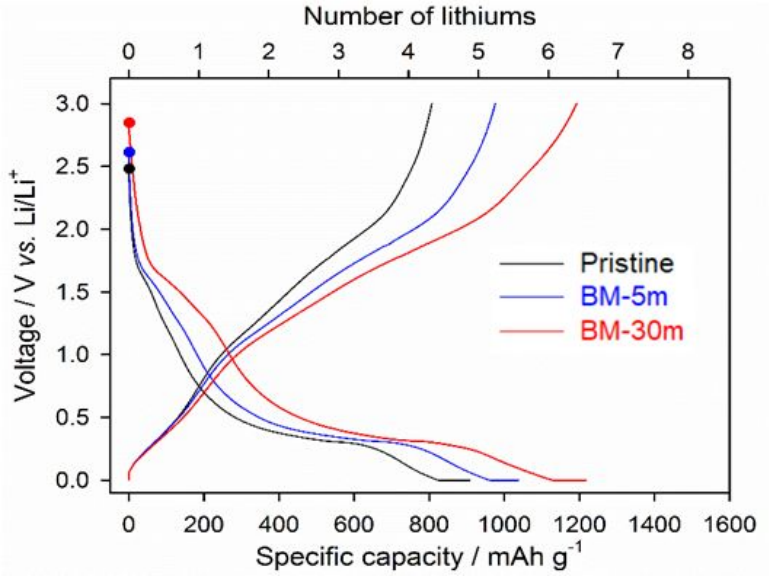

Figure S2. Second-cycle galvanostatic voltage profiles of pristine, BM-5m, and BM-30m electrodes. The circles indicate the initial voltages for the second cycle (2.48 V, 2.61 V and 2.85 V (*vs.* Li/Li^+), for pristine, BM-5m, and BM-30m, respectively).

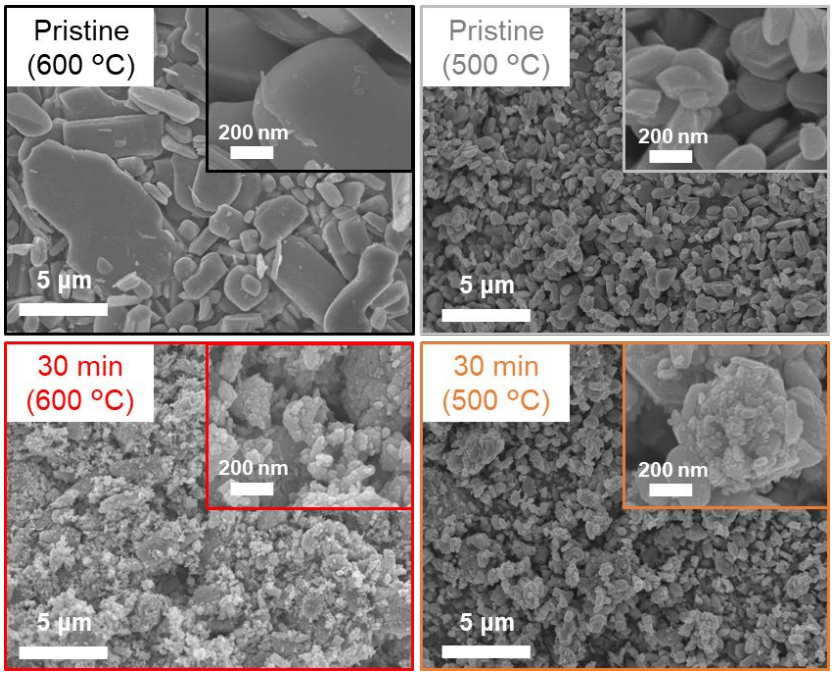

Figure S3. FE-SEM images of the pristine and 30 min ball-milled MoO_3 powders, synthesized at 600 °C and 500 °C.

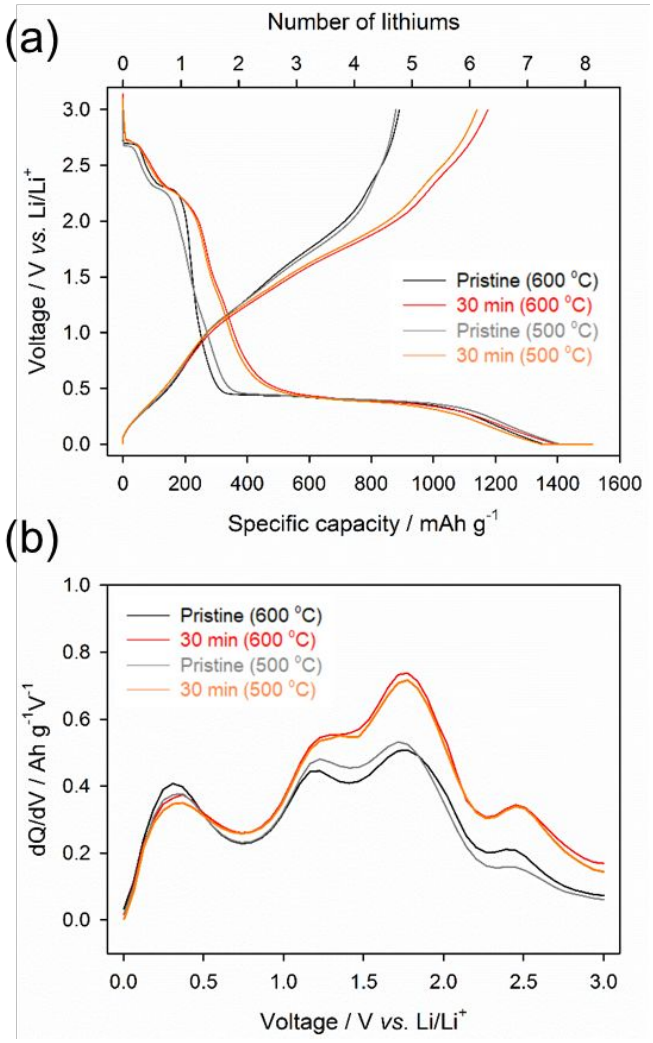

Figure S4. (a) First-cycle galvanostatic voltage profiles and (b) delithiation dQ/dV plots of the pristine and 30 min ball-milled MoO_3 electrodes, synthesized at 600 °C and 500 °C.

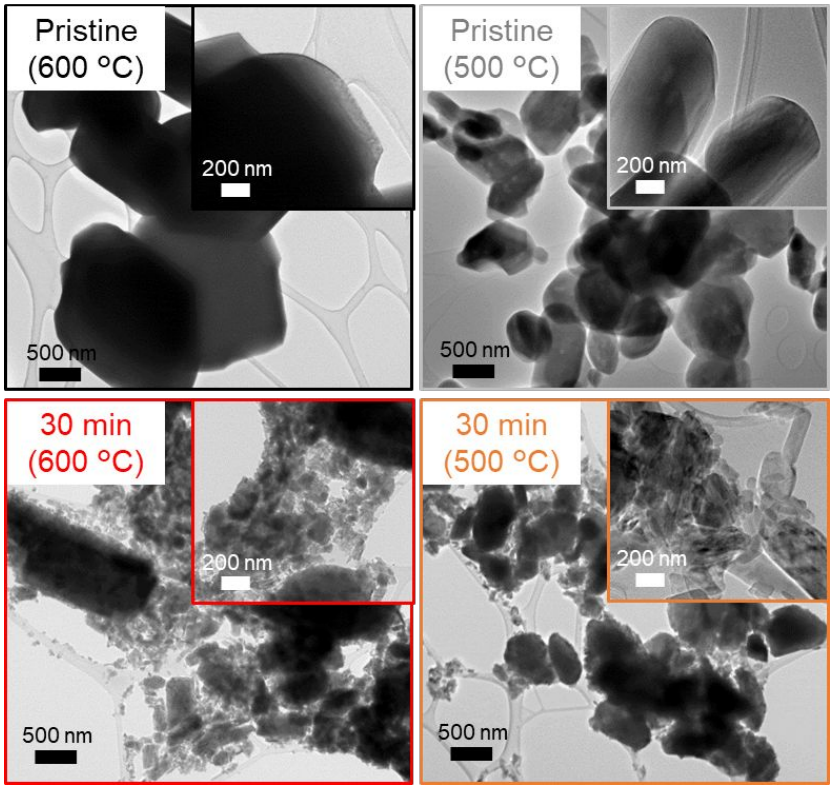

Figure S5. TEM images of the pristine and 30 min ball-milled MoO_3 powders, synthesized at 600 °C and 500 °C.

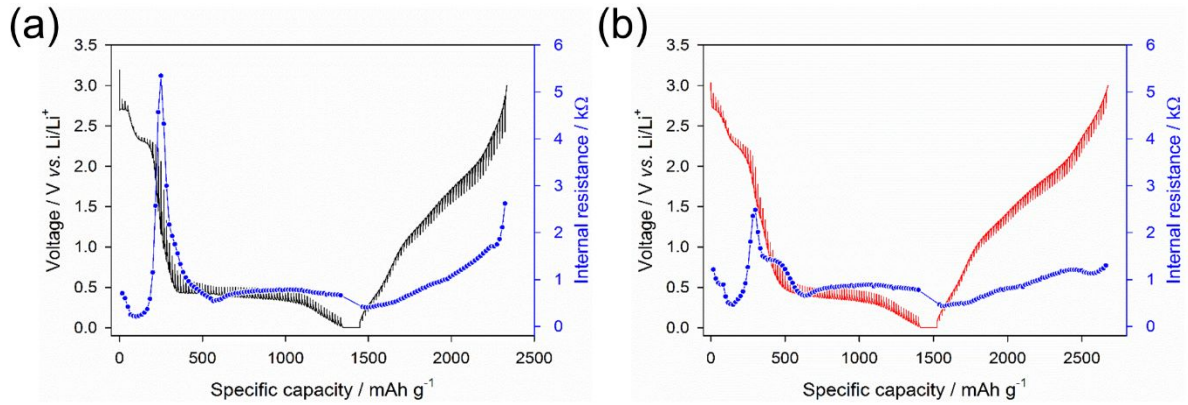

Figure S6. The GITT of (a) pristine MoO_3 and (b) BM-30m samples during the first cycle.

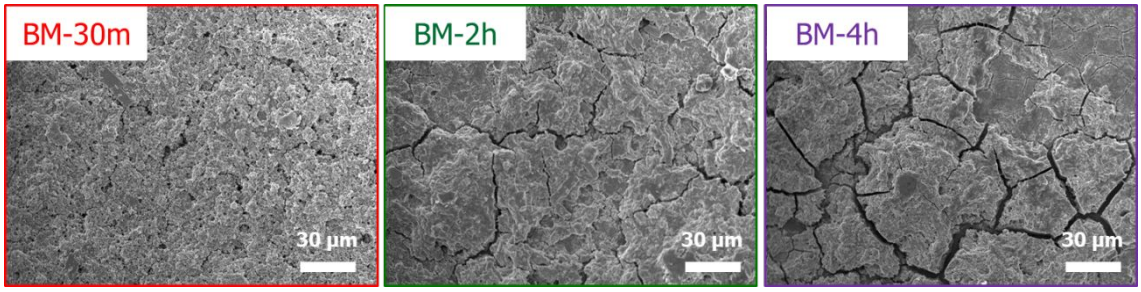

Figure S7. Low magnification FE-SEM images of the BM-30m, BM-2h, and BM-4h electrodes. Notably, there are severe cracks in the BM-2h and BM-4h electrodes, which were formed due to the water solubility of MoO_{3-x}.

Table S1. The governing equation, initial and boundary conditions, and parameters used to simulate the concentration gradient of lithium ion in MoO_3 particles.

	Mass balance equation Initial & Boundary conditions Parameters
Mass balance	$\frac{\partial C}{\partial t} = D\nabla^2 C$
Initial condition	$C(0,r) = C_0 \; at \; t = 0$
Boundary condition	$\frac{\partial C}{\partial r} = 0 \;\; at \; r = 0$ $D\frac{\partial C}{\partial r} = -\frac{I \cdot V \cdot \rho}{F \cdot A} \;\; at \; r = R$
Diffusion coefficient	$D = 1.5 \times 10^{-17}$ m^2 s^{-1}
Initial concentration	$C_0 = 0.1117$ mol cm^{-3}
Current density	$I = 100$ mA g^{-1}
Particle volume and area	$V = \frac{4}{3}\pi R^3, \qquad A = 4\pi R^2$
Radius	$R = 10$ nm (or 1 μm)
Density	$\rho = 4.69$ g cm^{-3}
Faraday constant	$F = 96485$ C mol^{-1}

Table S2. First-cycle lithiation, delithiation, and the Coulombic efficiency of pristine MoO_3, BM-5m, BM-30m, BM-2h, and BM-4h electrodes.

First cycle	Lithiation capacity (mAh g^{-1})	Delithiation capacity (mAh g^{-1})	Coulombic efficiency (%)
Pristine	1465	890	60.8
BM-5m	1454	1010	69.5
BM-30m	1503	1176	78.2
BM-2h	1442	1057	73.3
BM-4h	1463	648	44.3

Table S3. Initial Coulombic efficiency of 30 min ball-milled MoO_3 electrodes with various ball-milling conditions: speed and ball-to-powder ratios.

Initial Coulombic efficiency (%)		Ball-milling speed (rpm)			
		100	200	300	400
Ball to powder ratio	Bare	60.8			
	5 : 1	-	-	62.1	-
	10 : 1	60.8	63.6	70.6	76.1
	20 : 1	62.0	74.4	78.2	78.0
	40 : 1	-	75.0	75.5	-